

Latent Reconstruction-Aware Variational Autoencoder

Onur Boyar¹ Ichiro Takeuchi^{1,2}

Abstract

Variational Autoencoders (VAEs) have become increasingly popular in recent years due to their ability to generate new objects such as images and texts from a given dataset. This ability has led to a wide range of applications. While standard tasks often require sampling from high-density regions in the latent space, there are also tasks that require sampling from low-density regions, such as Morphing and Latent Space Bayesian Optimization (LS-BO). These tasks are becoming increasingly important in fields such as de novo molecular design, where the ability to generate diverse and high-quality chemical compounds is essential. In this study, we investigate the issue of low-quality objects generated from low-density regions in VAEs. To address this problem, we propose a new VAE model, the Latent Reconstruction-Aware VAE (LRA-VAE). The LRA-VAE model takes into account what we refer to as the Latent Reconstruction Error (LRE) of the latent variables. We evaluate our proposal using Morphing and LS-BO experiments, and show that LRA-VAE can improve the quality of generated objects over the other approaches, making it a promising solution for various generation tasks that involve sampling from low-density regions.

1. Introduction

Deep generative models can generate synthetic complex objects such as images, texts, and chemical compounds by effectively learning their latent representations. The variational auto-encoder (VAE) is one of the most popular deep generative models. A VAE consists of two deep neural networks (DNNs): an encoder network that maps input instances to a low-dimensional latent space, and a decoder network that maps latent variables back to the original input object space. The main idea behind the VAE is to learn a probabilistic model of the input object distribution by

training the encoder and decoder networks. After training a VAE, it is possible to generate synthetic objects by sampling from the latent space and passing them through the decoder network.

In the VAE, objects generated by sampling from high-density regions of the latent variable distribution are of high quality, whereas those generated by sampling from low-density regions are of low quality. For example, Fig. 1 shows examples of synthetic images generated from high-density and low-density regions of the latent variable distribution using the VAE trained on the Fashion MNIST dataset (Xiao et al., 2017). Although standard generation tasks require sampling mainly from high-density regions, more advanced tasks that we consider in this study require sampling also from low-density regions.

This study is motivated from one of such an advanced task called *Latent Space Bayesian Optimization (LS-BO)*. LS-BO is a method for optimizing a black-box (BB) function using a Bayesian surrogate model constructed in the LS of a deep generative model such as the VAE. The main advantage of LS-BO is that optimization of high-dimensional complex objects such as chemical compounds can be performed in a latent lower-dimensional vector space. Although LS-BO has been actively studied in various fields, it has been pointed out that the objects suggested by LS-BO are often of low quality and lack diversity. As we demonstrate it later, the low quality objects are generated when an LS-BO explores low-density regions in the LS.

In this study, we introduce a simple yet effective novel approach, *Latent Reconstruction-Aware VAE (LRA-VAE)*, to improve the quality of synthetic objects sampled from low-density regions in LSs. Our basic idea is to consider, what we call, *Latent Reconstruction Error (LRE)*. To define the LRE, let us denote the encoder and decoder networks of a trained VAE as $f_{\phi}^{\text{enc}} : \mathbf{x} \mapsto \mathbf{z}$ and $f_{\theta}^{\text{dec}} : \mathbf{z} \mapsto \mathbf{x}$, respectively, where $\mathbf{x} \in \mathcal{X}$ is an input objects in the input domain (denoted by \mathcal{X}), whereas $\mathbf{z} \in \mathcal{Z}$ is the latent variable in the LS (denoted by \mathcal{Z}), and ϕ and θ are the parameters of the encoder and decoder networks, respectively. For a latent variable $\mathbf{z} \in \mathcal{Z}$, the LRE is defined as

$$\text{LRE}(\mathbf{z}) = \|\mathbf{z} - \hat{\mathbf{z}}\|^2, \quad (1)$$

where we used the $\hat{}$ notation to indicate a variable that is

¹Nagoya University ²RIKEN. Correspondence to: Ichiro Takeuchi <ichiro.takeuchi@mae.nagoya-u.ac.jp>.

reconstructed back by using both the encoder and decoder networks of a trained VAE, namely $\hat{z} = f_{\phi}^{\text{enc}}(f_{\theta}^{\text{dec}}(z))$. The details of f_{ϕ}^{enc} and f_{θ}^{dec} are described in §2. Our idea is to simply minimize the loss function of a VAE along with LREs for a set of latent variables sampled from a probability distribution defined on the LS, which we call, *latent reference distribution* and denote it as p_{ref} . The proposed LRA-VAE is formulated by adding an extra term $\mathbb{E}_{p_{\text{ref}}}[\text{LRE}(z)]$ to the objective function of the standard VAE (see (2) in §2 and (3) in §3), where $\mathbb{E}_{p_{\text{ref}}}[\cdot]$ is the expectation operator in terms of the probability law p_{ref} .

The proposed LRE-VAE is beneficial not only in LS-BO but also in other tasks by considering various choices of latent reference distribution $p_{\text{ref}}(z)$. Specifically, we consider the following two types of choices of latent reference distribution. The first type is for cases where we want to improve the quality of the generated objects *in general*. Specifically, we consider the case where $p_{\text{ref}}(z)$ is chosen to cover the support of the prior distribution of the latent variables of the VAE. When the prior distribution is set to be a multivariate standard normal distribution, the latent reference distribution may be set to be a multivariate normal distribution $N(\mathbf{0}, \sigma_{\text{ref}} I)$, where $\mathbf{0}$ is a vector of 0, $\sigma_{\text{ref}} \geq 1$ is a scalar, and I is the identity matrix. We demonstrate that this choice improves the quality of the objects even when they are generated from low-density regions in the LS.

The second type of latent reference distribution is for cases where we are interested in particular regions in the LS. An example is the setting where we want to generate new objects through interpolation or extrapolation in the LS. This setting arises in *morphing* task which is the process of smoothly transitioning from one object to another by interpolating the LS representation of the two objects, or further exploring the LS by extrapolating to a particular direction in the LS. Another example arises in the LS-BO task described above. In the LS-BO, the regions of interests are determined by an *Acquisition Function* (AF) of the employed BO algorithm. For both tasks, when the regions of interest are in the low-density regions, the generated objects could be of low-quality. Figure 1c shows synthetic images generated by the LRA-VAE when they are sampled from the same low-density regions as those in Fig. 1b. It can be observed that the qualities of the generated images are improved when the LRA-VAE is used.

The main contributions of this study are summarized below.

1. We propose a simple yet effective approach, *Latent Reconstruction-Aware VAE (LRA-VAE)*, that can improve the quality and diversity of generated objects even when they are sampled from low-density regions in the LS.
2. We demonstrate that the proposed LRA-VAE can im-

prove the quality of VAE as a generative model. Specifically, we demonstrate through numerical experiments that the LRA-VAE improves the quality and diversity of the generated objects.

3. We consider two specific scenarios where LRA-VAE can be effectively used. Specifically, we propose methods to improve the quality and diversity of objects generated in LS morphing and in LS-BO using the LRA-VAE approach.

1.1. Related Works

The VAE (Kingma & Welling, 2014) is one of the most popular generative models with many application domains. The original objective of the VAE is to learn the distribution of the input objects and generate input like objects. VAEs have been used for many tasks such as image generation (Razavi et al., 2019), anomaly detection (Xu et al., 2018), and denoising tasks (Im et al., 2017). VAEs are also useful for generating objects by performing interpolation or extrapolation in the LS. Oring et al. (2021) and Berthelot et al. (2018) proposed regularization technique to resolve the problem of performing interpolation on the LS. Cristovao et al. (2020) proposed adding a penalization term to the objective function of VAEs to penalize poor interpolations. Liu et al. (2018) utilized data augmentation and an adversarial loss to improve interpolations.

The BO (Shahriari et al., 2016; Frazier, 2018) is a BB function optimization technique that is particularly useful when the cost of the BB function evaluation is high. It has been recognized that BOs perform poorly in high-dimensional problems. One way to tackle this problem is to learn a low dimensional vector representation of the objects and run a BO in the low dimensional space. The VAE is one of the options to learn the low dimensional representation, and its generative capabilities make it one of the best options to use in BO, which is called LS-BO. LS-BOs are used in many different settings such as neural architecture search (Kandasamy et al., 2018; Zhou et al., 2019; Zhang et al., 2019), image generation (Berthelot et al., 2022), material discovery (Griffiths & Schwaller, 2018; Choudhary et al., 2022), and protein design (Hie & Yang, 2022).

This study is motivated by the *de novo molecular design* problem, whose aim is to find a chemical compound(s) with a desired chemical property. The LS-BO was first introduced to solve this problem in (Gómez-Bombarelli et al., 2018), where a simple combination of the standard VAE and the standard BO was considered. Griffiths & Hernández-Lobato (2020) proposed constrained BOs for avoiding generations of invalid chemical compounds. Gómez-Bombarelli et al. (2018) also considered training a VAE along with a label (i.e., chemical property) prediction model in the LS, whose aim is to shape the LS to be more suitable to la-



Figure 1. Visualization of synthetic images generated from **a)** high-density regions **b)** low-density regions using a standard VAE. **c)** Visualization of synthetic images generated from low-density regions using LRA-VAE. The details of the setup to produce these images are described in App. A.1.

bel predictions. As another approach to incorporate label information, Lim et al. (2018) proposed the use of a conditional VAE, whereas Richards & Groener (2022) suggested a conditional β -VAE. These methods are still sub-optimal because the new label information obtained through BO iteration(s) is not incorporated into the VAE. There are various works in which the VAE is retrained with label information obtained through BO iteration(s). Tripp et al. (2020) proposed a weighted retraining approach where the VAE is retrained by an updated training set after BO iteration(s), where the weights of the instances in the updated training set are set to be proportional to their label information. Grosnit et al. (2021) introduced a metric learning approach while retraining the VAE. Berthelot et al. (2022) proposed invariant data augmentations to improve the quality of the LS and make it more amenable to BO. Siivola et al. (2021) evaluated the impact of various settings such as latent dimension and the selection of AFs for LS-BO.

2. Preliminaries and Problem Definition

Here, we present preliminary information and problem definition.

2.1. VAEs

A VAE consists of an encoder network $f_\phi^{\text{enc}} : \mathcal{X} \rightarrow \mathcal{Z}$ and a decoder network $f_\theta^{\text{dec}} : \mathcal{Z} \rightarrow \mathcal{X}$ where \mathcal{X} is the domain of input variables (objects) \mathbf{x} and \mathcal{Z} is the domain of latent variables \mathbf{z} . In VAEs, input variables \mathbf{x} and latent variables \mathbf{z} are considered as random variables. Let $p_\theta(\mathbf{x})$ and $p_\theta(\mathbf{z})$ be the probability functions of \mathbf{x} and \mathbf{z} , respectively, where θ is the set of parameters for characterizing the probabilities¹. The encoder network f_ϕ^{enc} is formulated as a conditional probability $q_\phi(\mathbf{z} | \mathbf{x})$, which is considered as an approximation of $p_\theta(\mathbf{z} | \mathbf{x})$, whereas the decoder network f_θ^{dec} is formulated as a conditional probability $p_\theta(\mathbf{x} | \mathbf{z})$, where ϕ is the parameters of the encoder.

¹Note that the notation θ is also used as the parameters for the decoder network, and the reason for this will be clarified below.

The problem of training a VAE is formulated as the maximization of

$$J_{\text{VAE}}(\phi, \theta) = \mathbb{E}_{\mathbf{z} \sim q_\phi(\mathbf{z} | \mathbf{x})} \log p_\theta(\mathbf{x} | \mathbf{z}) - \beta D_{\text{KL}}(q_\phi(\mathbf{z} | \mathbf{x}) || p_\theta(\mathbf{z})), \quad (2)$$

where $\mathbb{E}_{\mathbf{z} \sim q_\phi(\mathbf{z} | \mathbf{x})}$ is an expectation operator for random variables \mathbf{z} that follows the conditional distribution $q_\phi(\mathbf{z} | \mathbf{x})$, $D_{\text{KL}}(\cdot || \cdot)$ is Kullback Leibler (KL) divergence between two distributions, and $\beta > 0$ is a hyperparameter to trade-off the balance between the two terms. In (2), the prior distribution of the latent variables $p_\theta(\mathbf{z})$ is usually set as a multivariate normal distribution $\mathcal{N}(\mathbf{0}, I)$. When $\beta = 1$, the objective function is reduced to that of the standard VAEs and it can be interpreted as a lower bound of the log likelihood of the input distribution $p_\theta(\mathbf{x})$. On the other hand, VAEs with $\beta \neq 1$ is called β -VAE (Higgins et al., 2016).

The conditional probability $q_\phi(\mathbf{z} | \mathbf{x})$ in the encoder network is formulated as follows. Given an input variable \mathbf{x} , the latent variable \mathbf{z} is encoded as $\mathbf{z} = \boldsymbol{\mu}_\phi(\mathbf{x}) + \sigma_\phi(\mathbf{x})\boldsymbol{\varepsilon}$, $\boldsymbol{\varepsilon} \sim \mathcal{N}(\mathbf{0}, I)$, where $\boldsymbol{\mu}_\phi : \mathcal{X} \rightarrow \mathcal{Z}$ and $\sigma_\phi : \mathcal{X} \rightarrow \mathbb{R}^+$ represent the mean and the standard deviation of the latent variable corresponding to \mathbf{x} , respectively, and they are implemented together in the encoder network f_ϕ^{enc} with the trainable parameters ϕ , whereas $\boldsymbol{\varepsilon}$ is a random variable sampled from $\mathcal{N}(\mathbf{0}, I)$. Using the conditional probability $p_\theta(\mathbf{x} | \mathbf{z})$ in the decoder network f_θ^{dec} , given a latent variable \mathbf{z} , an input variable $\hat{\mathbf{x}}$ is generated as $\hat{\mathbf{x}} \sim p_\theta(\mathbf{x} | \mathbf{z})$.

2.2. Morphing

In this study, we consider two tasks. The first task is *morphing*. Morphing refers to an *interpolation* between sets of points and *extrapolation* to certain directions in the LS \mathcal{Z} . Let \mathbf{x}_a and \mathbf{x}_b be two different input objects; and $\mathbf{z}_a = f_\phi^{\text{enc}}(\mathbf{x}_a)$ and $\mathbf{z}_b = f_\phi^{\text{enc}}(\mathbf{x}_b)$ be the corresponding two latent variables. Consider a set of parameterized latent variables $\mathbf{z}(\tau) = \tau \mathbf{z}_a + (1 - \tau) \mathbf{z}_b$, where τ is a scalar parameter with $\tau \in [0, 1]$ for interpolation and $\tau < 0$ or $\tau > 1$ for extrapolation. Using the decoder, a set of parameterized objects $\hat{\mathbf{x}}(\tau) = f_\theta^{\text{dec}}(\mathbf{z}(\tau))$ can be generated. They can be

interpreted as interpolations or extrapolations of the two input objects x_a and x_b . For example, in chemical compound design problems, we are interested in creating a chemical compound with an “intermediate” property between the two existing compounds x_a and x_b . We expect that such a new chemical compound can be generated by decoding an interpolated latent variable $z(\tau)$ between the two latent variables z_a and z_b .

2.3. LS-BO

The second task is LS-BO. In this task, we consider a situation where a large number of *unlabeled* instances $\{x_i\}_{i \in [\mathcal{U}]}$ and a small number of *labeled* instances $\{(x_i, y_i)\}_{i \in [\mathcal{L}]}$ are available, where $x_i \in \mathcal{X}$ is an input object such as chemical compound and $y_i \in \mathcal{Y} \subseteq \mathbb{R}$ is the label of the input object x_i such as drug-likeness of the chemical compound x_i . Here, the sets of indices of the unlabeled and labeled instances are denoted as \mathcal{U} and \mathcal{L} , respectively, and $\mathcal{Y} \subseteq \mathbb{R}$ indicates the space of the label which is assumed to be scalar in this study².

A BO is used for a BB function optimization problem when an evaluation of the BB function is expensive (in terms of time, money, etc.). Let us denote the BB function as $f^{\text{BB}} : \mathcal{X} \rightarrow \mathcal{Y}$. The goal of a BO is to find $x \in \mathcal{X}$ that maximizes the BB function with as small number of BB function evaluations as possible. The basic idea of BOs is to use a *surrogate model* for the BB function, and it is common to employ a *Gaussian Process (GP)* model as the surrogate model. If a good surrogate GP model on the input object space \mathcal{X} can be constructed using the labeled instances $\{(x_i, y_i)\}_{i \in \mathcal{L}}$, the predictive distribution of the label can be obtained for each input object with unknown labels. Using the predictive distributions, one or more candidates of input objects whose labels are predicted to be greater than the current maximum value $\max_{i \in \mathcal{L}} y_i$ can be selected. After evaluating the BB function for the candidate input objects, the labeled set \mathcal{L} and the GP surrogate model are updated. This process is repeated until we obtain the maximum value or use out the available resource budget.

Unfortunately, it is often difficult to develop a good GP surrogate model on the input object space \mathcal{X} when x is a high-dimensional complex object such as chemical compound. The basic idea of LS-BO is to first train a VAE using unlabeled set \mathcal{U} , and then fit a GP surrogate model on the LS \mathcal{Z} in the trained VAE. Fitting a GP model on the LS \mathcal{Z} can be easier than fitting it on the input object space \mathcal{X} because the former is lower-dimensional vector space. Let us denote a GP model in the LS by $f^{\text{GP}} : \mathcal{Z} \rightarrow \mathcal{Y}$ which is fitted by using $\{(f_\phi^{\text{enc}}(x_i), y_i)\}_{i \in \mathcal{L}}$. Furthermore, let us

denote the AF by $f^{\text{AF}} : \mathcal{Z} \rightarrow \mathbb{R}^+$ which is used to quantify how promising each candidate is for the BB function optimization problem. Among many choices of AFs, we use *Probability Improvement (PI)*, *Expected Improvement (EI)*, and *Upper Confidence Bound (UCB)* in this study.

At each iteration of LS-BO, by applying the AF to the predictive distributions obtained by the GP surrogate model on the LS, the latent variable that maximizes the AF, i.e., $z_{i'}^* = \arg\max_{z \in \mathcal{Z}} f^{\text{AF}}(z)$ can be obtained. Using the decoder, an input object to be evaluated as $x_{i'} = f_\theta^{\text{dec}}(z_{i'}^*)$ can be obtained. The labeled set is then updated as $\mathcal{L} \leftarrow \mathcal{L} \cup \{i'\}$ and the GP model is also updated accordingly. As in the standard BO, this process is repeated until we obtain the maximum value or use out the available resource budget. For example, in a chemical compound design problem, the LS-BO is used to find a chemical compound with desired property.

2.4. Difficulties and Challenges in Existing Methods

In both of the morphing and the LS-BO tasks, generation of objects from low-density regions in the VAE’s LS is required. In the morphing task, interpolated and extrapolated points in LS may be located in low-density regions where no training instances exist. In the LS-BO task, AFs often take large values in low-density regions for exploration purpose where no training instances exist. Since we are aiming in these tasks to generate *de novo* objects that are different from existing training instances, decoding from low-density regions in LS is an unavoidable fundamental issue.

The objective function of VAE was originally designed to generate objects similar to training input objects by randomly sampling from the prior distribution of latent variables. Therefore, if the LS identified by a VAE intend to be used for a different purpose, it is desirable to introduce a mechanism to modify a LS so that it is consistent with the new purpose. As described in §1, there have been several attempts to modify the VAE’s loss function for the LS to have some desired properties. The LRA-VAE proposed in this study is an attempt particularly useful for generating *de novo* objects.

3. Proposed Method: LRA-VAE

Here, we present our proposed approach, LRA-VAE. The LRA-VAE improves the quality of generated synthetic objects by incorporating the LREs into the objective function of the standard VAE.

3.1. Importance of LREs

Before introducing the LRA-VAE, let us explain why we pay attention to LREs for generating high-quality objects from low-density regions in a LS.

²In this study, although we consider regression problems and y is a scalar variable, we refer to it as a *label* in accordance with active learning terminology.

From our preliminary studies, we observed that LREs are high in low-density regions of LS. Figure 2 illustrates the relationships between LREs and the densities in the LSs of two VAEs trained on the Fashion MNIST and MNIST (Deng, 2012) datasets. Clearly, LREs in low-density regions are high, indicating that LREs might be an indicator of low-density regions and low-quality objects.

Additionally, we encountered the following practical issue in the LS-BO task. Consider a case where the AF in a LS-BO suggests a query $z^* \in \mathcal{Z}$. We then use the decoder to obtain $\hat{x}^* = f_{\theta}^{\text{dec}}(z^*)$ and the corresponding label $y^* = f^{\text{BB}}(\hat{x}^*)$ by evaluating the BB function f^{BB} on \hat{x}^* . When we update the GP surrogate model in the LS, there are two options. The first option is to update the GP with (z^*, y^*) as the new labeled instance as is done in earlier LS-BO studies, while another reasonable option is to update the GP with (\hat{z}^*, y^*) where $\hat{z}^* = f_{\phi}^{\text{enc}}(\hat{x}^*)$. We conjecture that the inconsistency between z^* and \hat{z}^* is a crucial issue in LS-BOs. As demonstrated in Fig. 3, z^* sampled from a low-density region is reconstructed back to \hat{z}^* in a high-density region in the LS. This suggests that, in LS-BOs, explorations of low-density regions are often difficult because we cannot actually generate new objects from unexplored low-density regions.

3.2. LRA-VAE

The objective function of the LRA-VAE is written as

$$J_{\text{VAE}}^{\text{LRA}}(\phi, \theta) = J_{\text{VAE}}(\phi, \theta) - \gamma \mathbb{E}_{z^* \sim p_{\text{ref}}(z^*)} [\text{LRE}(z^*)], \quad (3)$$

where $\gamma > 0$ is a hyperparameter to trade-off the balance between the two terms. Here, remember that $J_{\text{VAE}}(\phi, \theta)$ is the objective function of the standard VAE and $\text{LRE}(z^*) = \|z^* - \hat{z}^*\|^2$ with $\hat{z}^* = f_{\phi}^{\text{dec}}(z^*)$.

The implementation of the LRA-VAE is very simple — we can optimize (the parameters of) encoder f_{ϕ}^{enc} and decoder f_{θ}^{dec} of the VAE using an empirical version of the objective function in (3), where an extra term

$$\frac{1}{N^*} \sum_{i=1}^{N^*} \|z_i^* - \hat{z}_i^*\|^2 \simeq \mathbb{E}_{z^* \sim p_{\text{ref}}(z^*)} [\text{LRE}(z^*)]$$

is subtracted (with multiplication with γ) from the empirical objective function of the standard VAE. Here, $z_i^*, i \in [N^*]$, is a latent variable sampled from latent reference distribution p_{ref} , and N^* is the number the sampled latent variables³.

³Another possible definition of LREs is $\tilde{\text{LRE}}(z^*) = \mathbb{E}_{z^* \sim p_{\text{ref}}(z^*)} \left[\log \left(\frac{1}{\sqrt{2\pi\sigma_{\phi}^2(\hat{x})}} \right) \exp \left(-\frac{\|\mu_{\phi}(\hat{x}^*) - z^*\|^2}{2\sigma_{\phi}^2(\hat{x})} \right) \right]$,

where $\hat{x}^* = f_{\theta}^{\text{dec}}(z^*)$. Apart from the influence on $\sigma_{\phi}^2(\hat{x})$, this definition of LREs coincides with our current definition $\text{LRE}(z^*) = \|z^* - \hat{z}^*\|^2$ up to a constant.

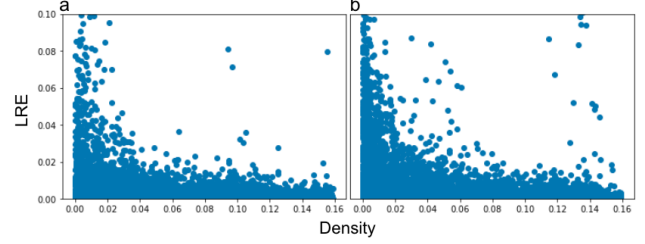


Figure 2. Densities of the test objects in the LS and their LREs using **a)** Fashion MNIST **b)** MNIST, which indicates a clear relationship between high LRE and low-density.

3.3. Latent Reference Distributions

In the LRA-VAE, the latent reference distribution p_{ref} can be arbitrarily specified according to the target task. In this study, we restrict our attention to the case where p_{ref} is a spherical multivariate normal distribution in the form of $N(\mu_{\text{ref}}, \sigma_{\text{ref}}^2 I)$, where $\mu_{\text{ref}} \in \mathcal{Z}$ and $\sigma_{\text{ref}} > 0$ are the mean vector and standard deviation, respectively. When we train an LRA-VAE, we can simply sample $z_i^* \sim N(\mu_{\text{ref}}, \sigma_{\text{ref}}^2 I), i \in [N^*]$. Adapting it to other choices of latent reference distributions is straightforward.

General Task: To address the general problem of obtaining low-quality objects from low-density regions in a LS, a reasonable choice is sampling from a normal distribution whose domain covers the domain of $p_{\theta}(z)$, the prior distribution of the latent variables. In the case where $p_{\theta}(z)$ is $N(0, I)$, we can set, e.g., $\mu_{\text{ref}} = 0$ and $\sigma_{\text{ref}} = 2$. On the other hand, if we are interested in a specific region, such as the region surrounding a specific latent variable $z^* \in \mathcal{Z}$, we could set $\mu_{\text{ref}} = z^*$ to decrease the LREs and improve the quality of the objects generated from that region. When we are interested in multiple regions, we can define the latent reference distribution to be a normal mixture distribution with equal mixing coefficients.

Morphing Task: In the morphing task, apart from defining a latent reference distribution like we described for the general task, we can specify the reference distribution to be a normal mixture distribution with the mean vectors of the mixture components being evenly aligned along with the parameterized line $z(\tau) = \tau z_a + (1 - \tau) z_b$ while the standard deviations and the mixture coefficients of all the components are the same.

LS-BO Task: In the LS-BO tasks, the regions of interest are naturally identified through the AF of BO, which locates the most promising regions in the LS. Decreasing the LREs in these regions can mitigate the negative effects of the inconsistency between z^* and \hat{z}^* in the LS on the GP fit for LS-BO tasks. This enables us with the LS-BO to search for unexplored low-density regions in the LS.

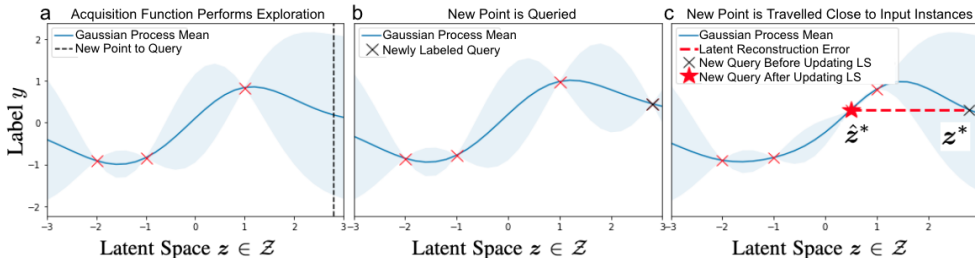


Figure 3. **a)** Next point to query is determined by the AF. **b)** New point is queried, appended to the training dataset, and the VAE is retrained. **c)** GP model is fitted on the updated LS in the retrained model. The red dashed line indicates the LRE of the queried point.

Algorithm 1 LS-BO with LRA-VAE

Input: pre-trained VAE, BB function: $f^{\text{BB}}(x)$, Unlabeled instances: $\mathcal{U} = \{\mathbf{x}_i\}_{i \in [\mathcal{U}]}$, Labeled instances: $\mathcal{L} = \{(\mathbf{x}_i, y_i)\}_{i \in [\mathcal{L}]}$, $f^{\text{AF}}(\mathbf{z})$, ReTraining Iteration: N , Standard Deviation of p_{ref} : σ_{ref} , Sample size of \mathbf{z}^* : N^*

repeat

- Fit GP model using $\{(f_{\phi}^{\text{enc}}(\mathbf{x}_i), y_i)\}_{i \in \mathcal{L}}$
- Run BO on latent space using GP model
- Obtain $\arg\max_{\mathbf{z} \in \mathcal{Z}} f^{\text{AF}}(\mathbf{z})$ and set $\mu_{\text{ref}} \leftarrow \arg\max_{\mathbf{z} \in \mathcal{Z}} f^{\text{AF}}(\mathbf{z})$
- for** $j = 1$ **to** N **do**
- Obtain samples $\{\mathbf{z}_i^*\}_{i \in [N^*]} \sim p_{\text{ref}}$
- ReTrain LRA-VAE using $\{\{\mathbf{x}_i\}_{i \in [\mathcal{U}]} \cup \{\mathbf{x}_i\}_{i \in [\mathcal{L}]}\}$ and $\{\mathbf{z}_i^*\}_{i \in [N^*]}$
- end for**
- Generate object: $\hat{\mathbf{x}}^* = f_{\theta}^{\text{dec}}(\mu_{\text{ref}})$
- Evaluate label: $y^* = f^{\text{BB}}(\hat{\mathbf{x}}^*)$
- Update: $\mathcal{L} \leftarrow \mathcal{L} \cup (\hat{\mathbf{x}}^*, y^*)$

until Query Budget is Reached

In the LS-BO tasks, it is common to use a pre-trained VAE model and update it based on new information obtained through BO, which is crucial as it allows incorporating new knowledge into the model to improve the efficiency of BO. Therefore, we have developed an algorithm that allows for the use of a pre-trained VAE model. Our proposed algorithm for using LRA-VAE for LS-BO tasks is outlined in Algorithm 1. After the AF identifies the point with the highest value to query, we set the center of latent reference distribution μ_{ref} to be that point, draw $\{\mathbf{z}_i^*\}_{i \in [N^*]}$, and retrain the LRA-VAE model. It is worth noting that at the first retraining iteration, the pre-trained VAE model is converted into an LRA-VAE model by adding the LRE to its objective function. Once the retraining iteration limit is reached, we obtain $\hat{\mathbf{x}}^* = f_{\theta}^{\text{dec}}(\mu_{\text{ref}})$ and $y^* = f^{\text{BB}}(\hat{\mathbf{x}}^*)$, and then append a new instance (μ_{ref}, y^*) to the labeled training set for the GP surrogate model in the LS.

4. Numerical Experiments

Here, we evaluated the performance of the proposed LRA-VAE approach through numerical experiments.

4.1. Datasets and Evaluation Metrics

General and Morphing Tasks: To illustrate the performances of standard VAE and LRA-VAE in general and morphing tasks, we used the Fashion MNIST dataset. We set $p_{\theta}(\mathbf{z})$ to be $\mathcal{N}(\mathbf{0}, I)$, for both the standard VAE and the LRA-VAE. In LRA-VAE, N^* is set to match the batch size of the input instances in each batch. We used models with a two-dimensional LS in order to easily visualize and analyze the latent variables and their latent reconstructions. As evaluation metrics, we used the LRE in (1), as well as the *Frechet Inception Distance (FID) Score* (Heusel et al., 2017) to measure the quality of generated objects. The details of FID Score is described in App. A.2.

LS-BO tasks: In the LS-BO task, we used the QM9 chemical compound dataset (Ruddigkeit et al., 2012; Ramakrishnan et al., 2014), which is a widely used benchmark dataset in de novo chemical design tasks. To represent chemical compounds, we used the SELFIES representation (Krenn et al., 2020) as it has improved validity properties compared to more commonly used SMILES representation (Weininger, 1988). Using SELFIES representation allowed us to train our models without introducing any grammatical rules to address validity concerns for generated chemical compounds (Jin et al., 2018; Kajino, 2019). We used the similar VAE architecture as in (Krenn et al., 2020) with a three-dimensional LS. To train the GP model, we used 500 labeled training instances. Furthermore, in each batch, N^* was set to half of the batch size of the input instances.

The goal of LS-BO task considered in this experiment was to generate a chemical compound with a high *Penalized LogP (PLogP)* score. We used RDKit⁴ open-source software to calculate PLogP values, following the calculation method applied in (Tripp et al., 2020). We conducted experiments

⁴<https://www.rdkit.org/>

Table 1. LREs of the models trained using the Fashion MNIST dataset. Sample Dist. indicates the distribution that is used to generate random samples with sample size 10000.

SAMPLE DIST.	VAE LRE	LRA-VAE LRE
$\mathcal{N}(\mathbf{0}, I)$	0.047	0.019
$\mathcal{N}(\mathbf{1}, I)$	0.202	0.029
$\mathcal{N}(\mathbf{2}, I)$	0.772	0.065
$\mathcal{N}(\mathbf{3}, I)$	1.975	0.201

Table 2. FID score values of the generated synthetic objects.

SAMPLE DIST.	MODEL	FID
$\mathcal{N}(\mathbf{2}, I)$	VAE	187.22 ± 2.49
	LRA-VAE	157.36 ± 3.87
$\mathcal{N}(\mathbf{3}, I)$	VAE	228.57 ± 2.18
	LRA-VAE	192.04 ± 3.28
$\mathcal{N}(\mathbf{4}, I)$	VAE	268.3 ± 2.64
	LRA-VAE	194.76 ± 2.4

using three different AFs introduced in §2, i.e., EI, PI, and UCB.

4.2. Results

General Tasks: We conducted various experiments to evaluate the quality of the generated objects and compared LREs of the VAE and the LRA-VAE across different regions of LS. We accomplished this by varying the latent reference distribution. This allowed us to gain insight into how the performance change according to the density of the LS region. In the LRA-VAE, the latent reference distribution parameters were set to $\mu_{\text{ref}} = \mathbf{0}$ and $\sigma_{\text{ref}} = 2$.

The LREs for objects with different sampling locations are shown in Table 1. As evident from the table, LREs increase as the center of the sampling locations moves further away from $p_{\theta}(z)$ for both the VAE and the LRA-VAE. However, for each sampling distribution, the LREs of the LRA-VAE are lower than those of the VAE. Furthermore, we observed that the relative difference between LREs between the VAE and the LRA-VAE increases as the density of the sampling region decreases.

Next, we evaluated the quality of synthetic objects generated from low-density regions by calculating FID scores. We generated 100 sets of 1000 latent variables for each sampling region using the VAE and the LRA-VAE. We used the same LRA-VAE model as we used for above experiments, where $\mu_{\text{ref}} = \mathbf{0}$ and $\sigma_{\text{ref}} = 2$. As observed in Table 2, the FID scores of the objects obtained by LRA-VAE are consistently lower than those of the VAE across different regions in the LS, indicating improved quality by the LRA-VAE.

Morphing: Having observed the improved quality and de-

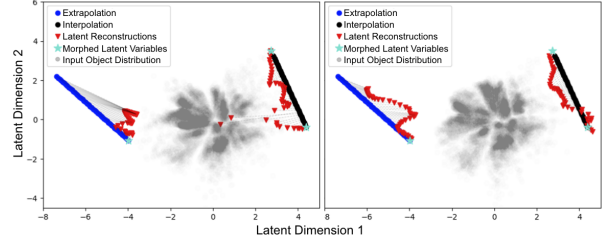


Figure 4. LS visualization of the morphing tasks of the a) VAE b) LRA-VAE.

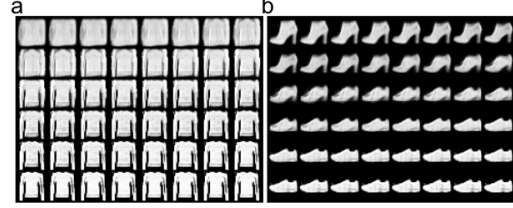


Figure 5. a) Extrapolated images using the VAE. b) Extrapolated images using the LRA-VAE.

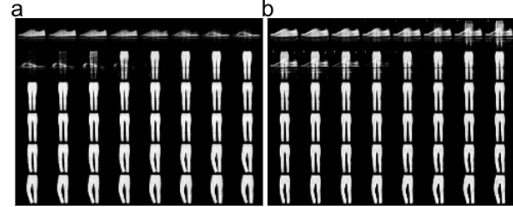


Figure 6. a) Interpolated images using VAE. b) Interpolated images using LRA-VAE.

creased LRE with the LRA-VAE, we proceed with the experiments on morphing in the LS. We identified pairs of latent representations of input objects from low-density regions and performed extrapolation and interpolation tasks using the VAE and the LRA-VAE. We subsequently analyzed and compared the quality of the generated synthetic objects and LREs in these experiments.

For both extrapolation and interpolation tasks, we used the LRA-VAE with latent reference distribution with $\mu_{\text{ref}} = \mathbf{0}$ and $\sigma_{\text{ref}} = 2$. For extrapolation task, we set $\tau \in (-0.02, -0.04, \dots, -0.98, -1, 0)$, and we incremented τ by 0.02 in $[0, 1]$ for interpolation task.

The morphed latent variables for both the VAE and the LRA-VAE (shown in blue for extrapolation and shown in black for interpolation) and their corresponding latent reconstructions (shown in red) are illustrated in Fig. 4. The gray regions in these plots refer to the input object distribution in the LS, and the turquoise points refer to the latent representations of the input objects used in morphing tasks. In Fig. 4a, we observe in the results of the VAE, the latent reconstructions

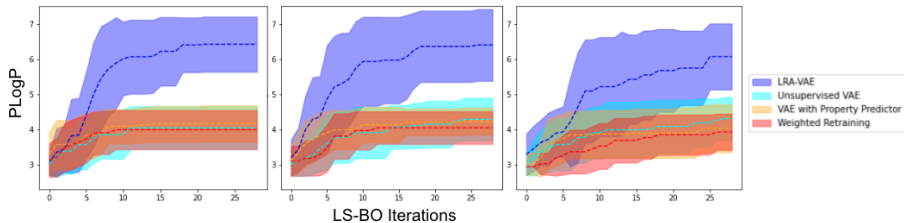


Figure 7. LS-BO results of different approaches using a) EI, b) PI c) UCB.

sometimes travel close to the input object distribution. On the other hand, the results of the LRA-VAE (Fig. 4b) clearly shows that the magnitude of LREs is smaller and the reconstructions by the LRA-VAE do not travel close to the input object distribution. An example set of generated images from extrapolation and interpolation experiments are shown in Figs. 5 and 6, respectively. Extrapolated images generated by the LRA-VAE (Fig. 5b) have good quality and a smooth transition between different styles of objects, while the VAE results (Fig. 5a) do not have the similar level of quality. The results indicate improved quality and decreased LREs in favor of LRA-VAE⁵. When it comes interpolated images (Fig. 6), while it may be difficult to discern a significant difference in image quality beyond the first and second row of the generated images, which are of better quality in favor of the LRA-VAE, the results suggest that the LRA-VAE can decrease the LREs without compromising sample quality.

LS-BO: Here, we use the LRA-VAE for LS-BO task as described in Algorithm 1.

To evaluate the effectiveness of the LRA-VAE, we compared it to other methods in the literature, including the unsupervised VAE and VAE with property predictor models proposed in (Gómez-Bombarelli et al., 2018), as well as the weighted retraining approach proposed in (Tripp et al., 2020). The first two methods are post-training techniques that do not update the VAE with new information obtained through BOs, whereas the last approach updates the VAE with new information.

In previous studies, the number of iterations in a LS-BO were relatively large, typically more than 100. However, in real-world scenarios, each iteration of BO requires conducting a new experiment, which incurs costs. To account for this constraint, we evaluated the performance of each approach under a limited budget of 30 LS-BO iterations. In the LRA-VAE, we set $\sigma_{\text{ref}} = \sqrt{0.2}$ to focus the z^* in the close vicinity of the region where $f^{\text{AF}}(z)$ is maximized.

To compare the performance of each approach, we conducted repeated experiments using different AFs listed in §4.1. The results in Fig. 7 demonstrate that our approach

⁵Further discussion on $f_{\theta}^{\text{dec}}(z^*)$ and $f_{\theta}^{\text{dec}}(\hat{z}^*)$ is provided in App.A.3.

Table 3. Highest TOP 3 PLogP values across all experiments.

MODEL	TOP 1	TOP 2	TOP 3
UNSUPERVISED VAE	4.74	4.45	4.15
VAE WITH PROP. PRED.	4.45	4.15	2.94
WEIGHTED-RETRAINING	4.45	4.15	3.84
LRA-VAE	6.72	5.89	5.32

consistently produced the highest PLogP values for the discovered chemical compounds across all AFs. Table 3 shows the highest top 3 PLogP values obtained by each model. These results indicate the advantage of the LRA-VAE.

The performance of the weighted-retraining approach failed to outperform other competitor models. We conjecture that this is because a few new instances are not sufficient to update the LS. Although we used the same amount of new instances as weighted-retraining, an important difference is that the LRA-VAE uses artificial instances, which are sampled at the surrounding of the new instance to be queried, and the LRE optimization allows us to incorporate those artificial instances into the model updating process. This helps the LRA-VAE to bring meaningful updates to the LS even when there are a limited number of new instances available.

5. Conclusion

In conclusion, this study evaluated the quality of objects generated from low-density regions in VAEs and found that they often have poor quality and high LREs. Improving the quality of these objects is crucial for tasks such as Morphing and LS-BO, as these tasks require sampling from low-density regions. To address this issue, we proposed the LRA-VAE. The LRA-VAE considers the LREs of the latent variables and incorporates it into the objective function of the standard VAE. The results of Morphing and LS-BO experiments demonstrate that the LRA-VAE can generate higher quality samples. Additionally, the LRA-VAE is easy to implement and offers flexibility in selecting the region to draw the latent variables z^* and the type of latent reference distribution. Overall, our study suggests that the LRA-VAE is a promising solution for various generation tasks that

involve sampling from low-density regions.

Acknowledgements

This work was partially supported by MEXT KAKENHI (20H00601), JST CREST (JPMJCR21D3, JPMJCR21D3), JST Moonshot R&D (JPMJMS2033-05), JST AIP Acceleration Research (JPMJCR21U2), NEDO (JPNP18002, JPNP20006) and RIKEN Center for Advanced Intelligence Project.

References

- Berthelot, D., Raffel, C., Roy, A., and Goodfellow, I. Understanding and improving interpolation in autoencoders via an adversarial regularizer. 07 2018.
- Berthelot, D., Raffel, C., Roy, A., and Goodfellow, I. High-dimensional bayesian optimization with invariance, 2022.
- Choudhary, K., DeCost, B., Chen, C., Jain, A., Tavazza, F., Cohn, R., WooPark, C., Choudhary, A., Agrawal, A., Billinge, S., Holm, E., Ong, S., and Wolverton, C. Recent advances and applications of deep learning methods in materials science. *npj Comput Mater*, 8, 2022.
- Cristovao, P., Nakada, H., Tanimura, Y., and Asoh, H. Generating in-between images through learned latent space representation using variational autoencoders. *IEEE Access*, 8:149456–149467, 2020. doi: 10.1109/ACCESS.2020.3016313.
- Deng, L. The mnist database of handwritten digit images for machine learning research. *IEEE Signal Processing Magazine*, 29(6):141–142, 2012.
- Frazier, P. A tutorial on bayesian optimization. *ArXiv*, abs/1807.02811, 2018.
- Griffiths, R.-R. and Hernández-Lobato, J. M. Constrained bayesian optimization for automatic chemical design using variational autoencoders. *Chem. Sci.*, 11:577–586, 2020. doi: 10.1039/C9SC04026A. URL <http://dx.doi.org/10.1039/C9SC04026A>.
- Griffiths, R.-R. and Schwaller, P. Dataset bias in the natural sciences: A case study in chemical reaction prediction and synthesis design. *ArXiv*, abs/2105.02637, 2018.
- Grosnit, A., Tutunov, R., Maraval, A. M., Griffiths, R.-R., Cowen-Rivers, A. I., Yang, L., Zhu, L., Lyu, W., Chen, Z., Wang, J., Peters, J., and Bou-Ammar, H. High-dimensional bayesian optimisation with variational autoencoders and deep metric learning. *ArXiv*, abs/2106.03609, 2021.
- Gómez-Bombarelli, R., Wei, J. N., Duvenaud, D., Hernández-Lobato, J. M., Sánchez-Lengeling, B., Sheberla, D., Aguilera-Iparraguirre, J., Hirzel, T. D., Adams, R. P., and Aspuru-Guzik, A. Automatic chemical design using a data-driven continuous representation of molecules. *ACS Central Science*, 4(2):268–276, 2018. doi: 10.1021/acscentsci.7b00572.
- Heusel, M., Ramsauer, H., Unterthiner, T., Nessler, B., and Hochreiter, S. Gans trained by a two time-scale update rule converge to a local nash equilibrium. In *Proceedings of the 31st International Conference on Neural Information Processing Systems, NIPS’17*, pp. 6629–6640, Red Hook, NY, USA, 2017. Curran Associates Inc. ISBN 9781510860964.
- Hie, B. L. and Yang, K. K. Adaptive machine learning for protein engineering. *Current Opinion in Structural Biology*, 72:145–152, 2022. ISSN 0959-440X. doi: <https://doi.org/10.1016/j.sbi.2021.11.002>. URL <https://www.sciencedirect.com/science/article/pii/S0959440X21001457>.
- Higgins, I., Matthey, L., Pal, A., Burgess, C. P., Glorot, X., Botvinick, M. M., Mohamed, S., and Lerchner, A. beta-vae: Learning basic visual concepts with a constrained variational framework. In *International Conference on Learning Representations*, 2016.
- Im, D. I., Ahn, S., Memisevic, R., and Bengio, Y. Denoising criterion for variational auto-encoding framework. *Proceedings of the AAAI Conference on Artificial Intelligence*, 31(1), Feb. 2017. doi: 10.1609/aaai.v31i1.10777. URL <https://ojs.aaai.org/index.php/AAAI/article/view/10777>.
- Jin, W., Barzilay, R., and Jaakkola, T. Junction tree variational autoencoder for molecular graph generation. In *Proceedings of the 35th International Conference on Machine Learning*. PMLR, 02 2018.
- Kajino, H. Molecular hypergraph grammar with its application to molecular optimization. In Chaudhuri, K. and Salakhutdinov, R. (eds.), *Proceedings of the 36th International Conference on Machine Learning*, volume 97 of *Proceedings of Machine Learning Research*, pp. 3183–3191. PMLR, 09–15 Jun 2019. URL <https://proceedings.mlr.press/v97/kajino19a.html>.
- Kandasamy, K., Neiswanger, W., Schneider, J., Póczos, B., and Xing, E. P. Neural architecture search with bayesian optimisation and optimal transport. In *Proceedings of the 32nd International Conference on Neural Information Processing Systems, NIPS’18*, pp. 2020–2029, Red Hook, NY, USA, 2018. Curran Associates Inc.

- Kingma, D. P. and Welling, M. Auto-encoding variational bayes. In Bengio, Y. and LeCun, Y. (eds.), *2nd International Conference on Learning Representations, ICLR 2014, Banff, AB, Canada, April 14-16, 2014, Conference Track Proceedings*, 2014. URL <http://arxiv.org/abs/1312.6114>.
- Krenn, M., Häse, F., Nigam, A., Friederich, P., and Aspuru-Guzik, A. Self-referencing embedded strings (selfies): A 100% robust molecular string representation. *Machine Learning: Science and Technology*, 1(4):045024, oct 2020. doi: 10.1088/2632-2153/aba947. URL <https://dx.doi.org/10.1088/2632-2153/aba947>.
- Lim, J., Ryu, S., Kim, J., and Kim, W. Molecular generative model based on conditional variational autoencoder for de novo molecular design. *Journal of Cheminformatics*, 10, 07 2018. doi: 10.1186/s13321-018-0286-7.
- Liu, X., Zou, Y., Kong, L., Diao, Z., Yan, J., Wang, J., Li, S., Jia, P., and You, J. Data augmentation via latent space interpolation for image classification. In *2018 24th International Conference on Pattern Recognition (ICPR)*, pp. 728–733, 2018. doi: 10.1109/ICPR.2018.8545506.
- Oring, A., Yakhini, Z., and Hel-Or, Y. Autoencoder image interpolation by shaping the latent space. In Meila, M. and Zhang, T. (eds.), *Proceedings of the 38th International Conference on Machine Learning*, volume 139 of *Proceedings of Machine Learning Research*, pp. 8281–8290. PMLR, 18–24 Jul 2021. URL <https://proceedings.mlr.press/v139/oring21a.html>.
- Ramakrishnan, R., Dral, P., Rupp, M., and von Lilienfeld, A. Quantum chemistry structures and properties of 134 kilo molecules. *Scientific Data*, 1, 08 2014. doi: 10.1038/sdata.2014.22.
- Razavi, A., van den Oord, A., and Vinyals, O. Generating diverse high-fidelity images with vq-vae-2. In Wallach, H., Larochelle, H., Beygelzimer, A., d'Alché-Buc, F., Fox, E., and Garnett, R. (eds.), *Advances in Neural Information Processing Systems*, volume 32. Curran Associates, Inc., 2019. URL <https://proceedings.neurips.cc/paper/2019/file/5f8e2fa1718d1bbcadf1cd9c7a54fb8c-Paper.pdf>.
- Richards, R. and Groener, A. Conditional beta-vae for de novo molecular generation. 04 2022. doi: 10.26434/chemrxiv-2022-g3gvz.
- Ruddigkeit, L., van Deursen, R., Blum, L. C., and Reymond, J.-L. Enumeration of 166 billion organic small molecules in the chemical universe database gdb-17. *Journal of Chemical Information and Modeling*, 52(11):2864–2875, 2012. doi: 10.1021/ci300415d. URL <https://doi.org/10.1021/ci300415d>. PMID: 23088335.
- Shahriari, B., Swersky, K., Wang, Z., Adams, R. P., and de Freitas, N. Taking the human out of the loop: A review of bayesian optimization. *Proceedings of the IEEE*, 104 (1):148–175, 2016. doi: 10.1109/JPROC.2015.2494218.
- Siivola, E., Paleyes, A., González, J., and Vehtari, A. Good practices for bayesian optimization of high dimensional structured spaces. *Applied AI Letters*, 2, 05 2021. doi: 10.1002/ail.2.24.
- Szegedy, C., Vanhoucke, V., Ioffe, S., Shlens, J., and Wojna, Z. Rethinking the inception architecture for computer vision. In *2016 IEEE Conference on Computer Vision and Pattern Recognition (CVPR)*, pp. 2818–2826, 2016. doi: 10.1109/CVPR.2016.308.
- Tripp, A., Daxberger, E., and Hernández-Lobato, J. Sample-efficient optimization in the latent space of deep generative models via weighted retraining. In *Advances in Neural Information Processing Systems*, 06 2020.
- Weininger, D. Smiles, a chemical language and information system. 1. introduction to methodology and encoding rules. *Journal of Chemical Information and Computer Sciences*, 28(1):31–36, 1988. doi: 10.1021/ci00057a005. URL <https://doi.org/10.1021/ci00057a005>.
- Xiao, H., Rasul, K., and Vollgraf, R. Fashion-mnist: a novel image dataset for benchmarking machine learning algorithms. *ArXiv*, abs/1708.07747, 2017.
- Xu, H., Chen, W., Zhao, N., Li, Z., Bu, J., Li, Z., Liu, Y., Zhao, Y., Pei, D., Feng, Y., Chen, J., Wang, Z., and Qiao, H. Unsupervised anomaly detection via variational auto-encoder for seasonal kpis in web applications. In *Proceedings of the 2018 World Wide Web Conference, WWW '18*, pp. 187–196, Republic and Canton of Geneva, CHE, 2018. International World Wide Web Conferences Steering Committee. ISBN 9781450356398. doi: 10.1145/3178876.3185996. URL <https://doi.org/10.1145/3178876.3185996>.
- Zhang, M., Jiang, S., Cui, Z., Garnett, R., and Chen, Y. *D-VAE: A Variational Autoencoder for Directed Acyclic Graphs*. Curran Associates Inc., Red Hook, NY, USA, 2019.
- Zhou, H., Yang, M., Wang, J., and Pan, W. BayesNAS: A Bayesian approach for neural architecture search. In Chaudhuri, K. and Salakhutdinov, R. (eds.), *Proceedings of the 36th International Conference on Machine Learning*, volume 97 of *Proceedings of Machine Learning Research*, pp. 7603–7613. PMLR, 09–15 Jun 2019.

URL <https://proceedings.mlr.press/v97/zhoul9e.html>.

A. Appendix

A.1. Details of Figure 1

Here, we provide the specifics of the experimental setup that produced the results presented in Fig. 1.

First, we identified two regions that produced poor images, as shown in Fig. 1b, by decreasing the density of the sampling region gradually. To address the quality issues, we employed an LRA-VAE model with a normal mixture distribution as the latent reference distribution and the results in Fig. 1c were obtained. Different from morphing experiments, this experiment considers sampling region where there is no latent variable in the close vicinity of the sampling region. The mean vectors of the mixture distribution are set to the center of the lines for both of the sampling tasks visualized in Fig. 8. The standard deviations of each of the mixture components is set to identity matrices.

Fig. 8a shows that the LRE values of the VAE are significantly high. Using a mixture normal latent reference distribution in a region with such high LRE values requires careful tuning of the γ parameter. Setting $\gamma \geq 1$ negatively impacts the generative performance of the LRA-VAE model as it prioritizes reducing LRE values over learning the representations of the input objects. To strike a balance, we used a low value of γ hyperparameter, specifically $\gamma = 0.001$. As shown in Fig 8b, this results in a significant decrease in LRE values.

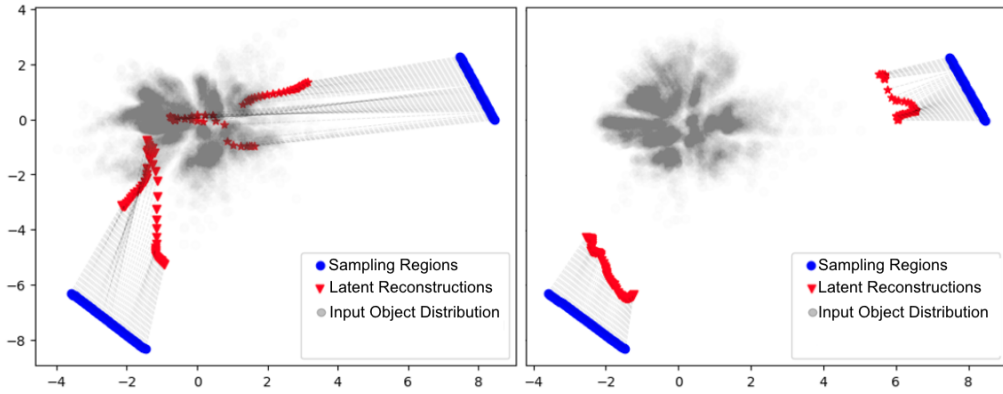


Figure 8. **a)** Sampling regions of the latent variables using the VAE and their latent reconstructions. **b)** Sampling regions of the latent variables using the LRA-VAE and their latent reconstructions.

A.2. FID Score

The FID Score is used to quantify the distance between real and synthetic objects by estimating their densities using the Inception v3 model (Szegedy et al., 2016). A high FID score indicates poor sample quality and a lack of diversity in the generated objects. The FID score is calculated as $FID = \|\mu_1 - \mu_2\|^2 + \text{Tr}(\Sigma_1 + \Sigma_2 - 2 * \sqrt{(\Sigma_1 * \Sigma_2)})$, where, μ_1 and Σ_1 refer to the distribution parameters for the real objects, while μ_2 and Σ_2 are the distribution parameters for the generated synthetic objects.

A.3. Generations from \hat{z}^*

We observed that the LRA-VAE exhibited superior performance in terms of both the LREs and the quality of generated instances. Another key property is the correspondence between the generated instances from the morphing task, $f_{\theta}^{\text{dec}}(z(\tau))$, and generations from their latent reconstructions, $f_{\theta}^{\text{dec}}(\hat{z}(\tau))$. This helps us to understand and compare the capacity of preserving the features of $f_{\theta}^{\text{dec}}(z(\tau))$ in $f_{\theta}^{\text{dec}}(\hat{z}(\tau))$ for VAE and LRA-VAE. For such a comparison, we calculated the average *Binary Cross-Entropy (BCE)* error between $f_{\theta}^{\text{dec}}(z(\tau))$ and $f_{\theta}^{\text{dec}}(\hat{z}(\tau))$ using the latent variables obtained from Extrapolation and Interpolation tasks. BCE error between $a \in [0, 1]$ and $b \in [0, 1]$ is calculated as

$$BCE(a, b) = -(a \log(b) + (1 - a) \log(1 - b)).$$

A desirable property is to observe that the characteristics of $f_{\theta}^{\text{dec}}(z(\tau))$ are mostly preserved in $f_{\theta}^{\text{dec}}(\hat{z}(\tau))$. The results, demonstrated in Table 4, show that LRA-VAE has a lower average BCE, indicating a better alignment and preservation of

Table 4. Average BCE error between $f_{\theta}^{\text{dec}}(\mathbf{z}(\tau))$ and $f_{\theta}^{\text{dec}}(\hat{\mathbf{z}}(\tau))$.

EXPERIMENT	VAE	LRA-VAE
EXTRAPOLATION	0.566	0.21
INTERPOLATION	0.157	0.139

features between $f_{\theta}^{\text{dec}}(\mathbf{z}(\tau))$ and $f_{\theta}^{\text{dec}}(\hat{\mathbf{z}}(\tau))$, compared to VAE.